Manipulating Electromagnetic Wave Polarizations by Anisotropic Metamaterials

Jiaming Hao,[1] Yu Yuan,[2] Lixin Ran,[2] Tao Jiang,[2] Jin Au Kong,[2,3] C. T. Chan,[4] and Lei Zhou[1,*]

[1]*Surface Physics Laboratory and Physics Department, Fudan University, Shanghai 200433, China*
[2]*The Electromagnetic Academy at Zhejiang University, Zhejiang University, Hangzhou 310027, China*
[3]*Research Laboratory of Electronics, Massachusetts Institute of Technology, Cambridge, Massachusetts 02139, USA*
[4]*Physics Department, Hong Kong University of Science and Technology, Clear Water Bay, Kowloon, Hong Kong, China*

We show that the polarization states of electromagnetic waves can be manipulated through reflections by an anisotropic metamaterial plate, and *all* possible polarizations (circular, elliptic, and linear) are realizable via adjusting material parameters. In particular, a linearly polarized light converts its polarization *completely* to the cross direction after reflection under certain conditions. Microwave experiments were performed to successfully realize these ideas and results are in excellent agreement with numerical simulations.

Polarization is an important characteristics of electromagnetic (EM) waves. It is always desirable to have full control of the polarization states of EM waves. Conventional methods to manipulate polarization include using optical gratings, dichroic crystals, or employing the Brewster and birefringence effects, etc. [1,2]. Here we propose an alternative approach based on metamaterials [3–6]. Metamaterials have drawn much attention recently due to many fascinating properties discovered, such as the negative refraction [4], the in-phase reflection [5], and the axially frozen modes [6], etc. Here, we show that a specific metamaterial reflector can be employed to manipulate the polarization state of an incident EM wave. In particular, a *complete conversion* between two independent linear polarizations is realizable under certain conditions. We show the physics to be governed by the unique reflection properties of the metamaterial, and we perform experiments and finite-difference-time-domain (FDTD) simulations to demonstrate these ideas in the microwave regime.

We start from studying a model system as shown in Fig. 1(a), which consists of an anisotropic homogeneous metamaterial layer (of a thickness d) with a dispersive relative permeability tensor $\overleftrightarrow{\mu}_2$ (with diagonal elements $\mu_{xx}, \mu_{yy}, \mu_{zz}$) and a relative permittivity ε_2, put on top of a perfect metal substrate (with $\varepsilon_3 \rightarrow -\infty$, $\mu_3 = 1$). We consider the reflection and refraction properties of the structure, when a monochromatic EM wave with a wave vector $\vec{k}_{in} = (\omega/c)[\sin\theta\cos\phi\hat{x} + \sin\theta\sin\phi\hat{y} + \cos\theta\hat{z}]$ and a given polarization strikes on the surface. According to the Maxwell equations, EM waves should satisfy $\vec{E} = -(c^2/\omega^2\varepsilon_2)\vec{k} \times [(\overleftrightarrow{\mu}_2^{-1}) \cdot (\vec{k} \times \vec{E})]$ inside the metamaterial layer with $\vec{k}$ the wave vector. Given k_x and k_y, the dispersion relation between ω and k_z is determined by $(\omega/c)^4\varepsilon_2^2 - (\omega/c)^2\varepsilon_2\sum_i(\mu_{ii}^{-1})(k^2 - k_i^2) + (k^2/2)\sum_{i\neq j\neq l}\mu_{ii}^{-1}\mu_{jj}^{-1}k_l^2 = 0$, where $i, j, l = x, y, z$. The above equation has four roots corresponding to two refracted waves propagating forwardly and backwardly. The solution inside the second

layer must be a linear combination of these four waves, manifesting the *birefringence* effect [1,7]. To match the boundary conditions, we must also expand the waves in other regions to linear combinations of four solutions, namely, the forward (backward) waves with s and p polarizations. The reflected beam thus generally consists of both s and p modes, even if the incident wave possesses one polarization. To solve these problems, we have extended the conventional 2×2 transfer-matrix-method (TMM) [8] to a 4×4 matrix version [6,7,9].

We performed numerical calculations based on the TMM assuming that $\mu_{xx} = 1 + 70/(12.71^2 - f^2)$, $\mu_{yy} = 1 + 22/(6.80^2 - f^2)$, $\mu_{zz} = 1$, $\varepsilon_2 = 1$, $d = 1.3$ mm, where f denotes the linear frequency measured in GHz. Suppose the incident wave is s polarized, $\vec{E}^{in} = \hat{e}_s^{(in)}e^{i(-\vec{k}_{in}\cdot\vec{r}+\omega t)}$, the reflected wave can be written as $\vec{E}^r = (r_{ss}\hat{e}_s^{(r)} + r_{sp}\hat{e}_p^{(r)})e^{i(-\vec{k}_r\cdot\vec{r}+\omega t)}$, where $\hat{e}_s^{(in)}$, $\hat{e}_s^{(r)}$, and $\hat{e}_p^{(r)}$ are the unit **E** vectors in different cases. We define a polarization conversion ratio (PCR) as PCR $= r_{sp}^2/(r_{ss}^2 + r_{sp}^2)$. Without absorption and diffractions, we get $r_{ss}^2 + r_{sp}^2 \equiv 1$, and thus PCR $= r_{sp}^2$. The calculated results of PCR are shown as solid lines in Fig. 2(a) for a normal incidence case with $\phi = 45°$ [10], and in Fig. 2(b) for $\theta = \phi = 45°$. We find the PCR to be strongly enhanced around two frequencies, ~12.7 and ~6.8 GHz, corresponding precisely to the two resonances at which μ_{xx} or μ_{yy} tends to infinity. In particular, for the normal incidence case studied in Fig. 2(a), our theory predicts that PCR $= 100\%$ at the two resonance frequencies, indicating that a linearly polarized light converts its polarization *completely* after the reflection.

In general, both s and p components exist inside the reflected beam. Define $\Delta\varphi_{sp}$ by $r_{sp}/r_{ss} = |r_{sp}/r_{ss}|e^{i\Delta\varphi_{sp}}$; we calculated $\Delta\varphi_{sp}$ versus frequency for the two cases studied in Fig. 2. From the results (solid lines) recorded in Fig. 3, we find that $\Delta\varphi_{sp}$ can take arbitrary values within [$-180°$, $180°$] depending on the frequency, indicating
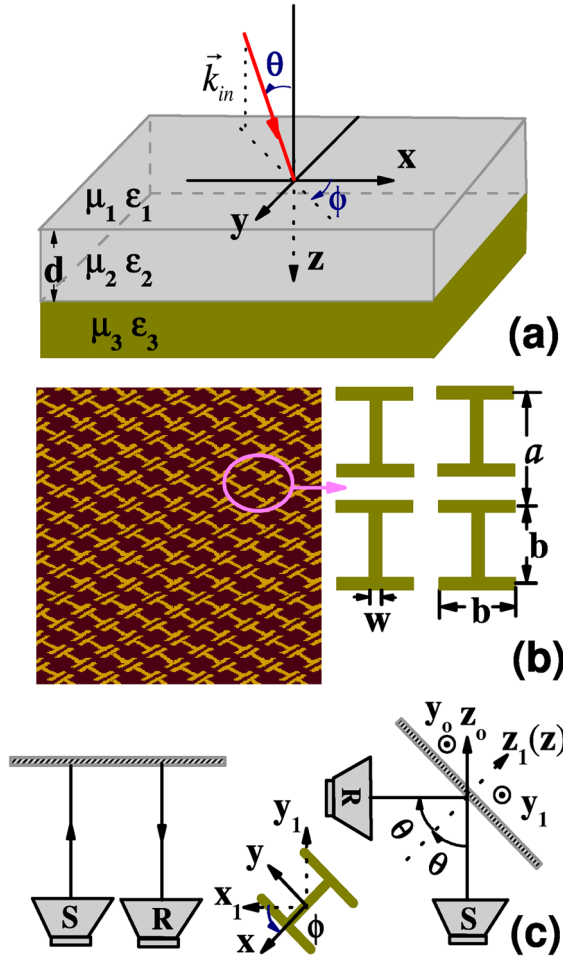
FIG. 1 (color online). (a) Geometry of the model system studied in this Letter. (b) Image of part of the experimental sample. (c) A schematic picture of the experiment setup. Starting from the laboratory coordinate system $\{\hat{x}_0, \hat{y}_0, \hat{z}_0\}$, we first rotate the sample for an angle of θ with respect to the $\hat{y}_0(=\hat{y}_1)$ axis, then for an angle of ϕ with respect to the $\hat{z}_1(=\hat{z})$ axis, and finally arrive at the local coordinate system $\{\hat{x}, \hat{y}, \hat{z}\}$ attached to the sample.

that all possible polarization states (circular, linear, elliptic) are realizable for the reflected beam. To illustrate, we chose four cases to calculate the polarization patterns of the reflected beams, and found that the resultant polarizations are linear (6.87 GHz), circular (7.27 GHz), and elliptic (10.9 and 12.46 GHz), correspondingly.

The physics can be understood by a simple argument. Consider the normal incidence case for simplicity. Suppose the incident wave is given by $\vec{E}^{\text{in}} = (E_x\hat{x} + E_y\hat{y})e^{i(-\omega z/c+\omega t)}$, then, after reflection by an ordinary material, the reflected wave is $\vec{E}^r = r(E_x\hat{x} + E_y\hat{y})e^{i(\omega z/c+\omega t)}$ with r the reflection coefficient. However, with anisotropy ($\mu_{xx} \neq \mu_{yy}$), the reflection coefficients, r_x, r_y are different for incident waves polarized along two directions. Thus, the reflected wave should be $\vec{E}^r = (r_xE_x\hat{x} + r_yE_y\hat{y})e^{i(\omega z/c+\omega t)}$ and the polarization state can be manipulated through varying r_x, r_y. For the configuration studied
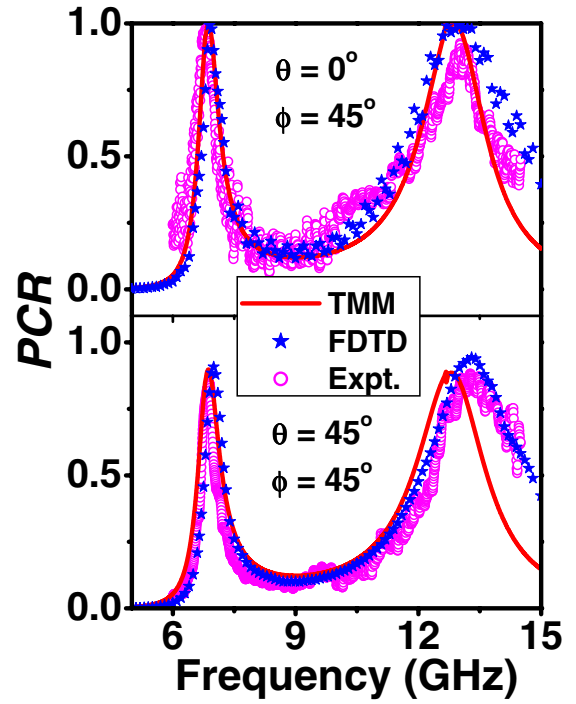

FIG. 2 (color online). PCR as the functions of frequency, obtained by TMM calculations on the model system (solid lines), FDTD simulations on realistic structures (solid stars), and experimental measurements (open circles). The incident direction is (a) $\theta = 0°$, $\phi = 45°$, and (b) $\theta = \phi = 45°$.

in Fig. 2(a) with $E_x = E_y$, if we tune the material parameters to yield $r_x/r_y = -1$, the polarization direction of the reflected wave would be $-\hat{x} + \hat{y}$, which is *perpendicular* to that of the original wave, $\hat{x} + \hat{y}$. A complete polarization conversion (CPC) is thus realized [11].

The key issue is then how to control r_x and r_y. With a metal plate on the back, our structure is always totally reflecting, i.e., $|r_x| = |r_y| \equiv 1$. However, the phase $\Delta\psi$ of the reflection coefficient, defined by $r_{x(y)} = e^{i\Delta\psi_{x(y)}}$, strongly depends on the metamaterial parameters. The calculated reflection phases ($\Delta\psi_x$, $\Delta\psi_y$) for the model system have been depicted in Fig. 4 versus frequency. In most cases where $\mu_{xx}(\mu_{yy})$ is not large, we have $\Delta\psi_{y(x)} \sim \pm 180°$, since the metamaterial layer is transparent and light can directly "see" the metal plate which is reflecting out of phase. However, at the resonances where $\mu_{xx}(\mu_{yy}) \to \pm\infty$, we get $\Delta\psi_{y(x)} = 0$ since light is reflected directly by the opaque metamaterial which possesses infinite impedance [5]. In general, we can obtain any value of $\Delta\psi_{y(x)}$ through adjusting the values of $\mu_{xx}(\mu_{yy})$ and d. The physics for the CPC effect is now clear. Near each resonance, one of μ_{xx}, μ_{yy} becomes very large while another close to 1, and there must be a frequency where $\Delta\psi_x - \Delta\psi_y = \pm 180°$ and thus $r_x/r_y = -1$ (see Fig. 4).

We study how the effect depends on the incident angles. Depicted in Fig. 5(a) are the PCR as functions of θ and ϕ, calculated at $f = 6.85$ GHz. Numerical computations re-
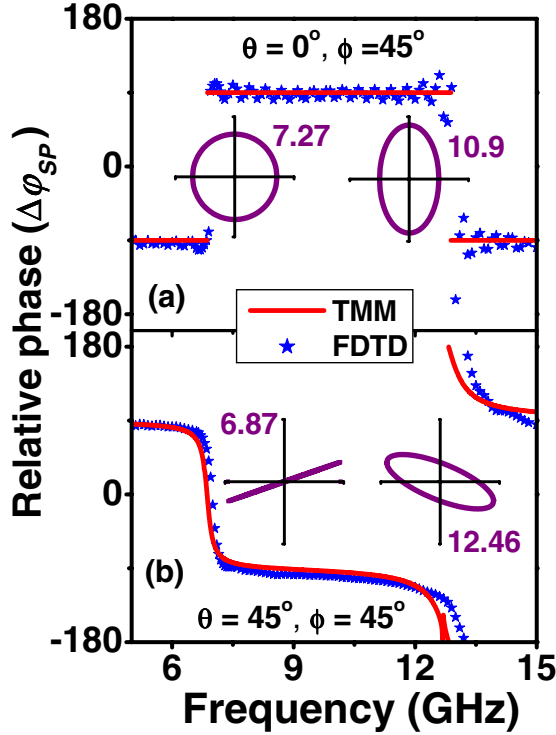
FIG. 3 (color online). Frequency dependence of the relative phase $\Delta\varphi_{sp}$ between the s- and p-polarized modes inside the reflected beam, calculated by TMM on model systems (solids lines) and FDTD simulations on realistic structures (solid stars). The incident direction is (a) $\theta = 0°$, $\phi = 45°$, and (b) $\theta = \phi = 45°$. The insets show the polarization patterns of the reflected beams calculated at different frequencies.

ior of ϕ was found for the resonance at $f = 12.7$ GHz. To facilitate easy comparisons with experiments, we show in Fig. 5(b) the PCR as a function of ϕ with $\theta = 45°$, and in Fig. 5(c) the PCR as a function of θ with $\phi = 45°$.

We employed experiments and FDTD simulations to demonstrate these predictions. To realize the proposed model system, we designed a frequency-selective structure as shown in Fig. 1(b), consisting of a periodic array of H-shaped metallic pattern (lattice constant $a = 7$ mm, thickness $= 0.1$ mm), printed on a 1.2 mm thick printed circuit board slab (with $\varepsilon_r = 3.6$) with a metal sheet on the back. Other parameters are fixed as $b = 5$ mm, $w = 1.0$ mm. A single H-shaped metallic structure possesses electric resonances for both polarizations [13]. When a metal plate is added, currents are induced on the metal plate surface, flowing along a direction *opposite* to the currents induced on the H structures. The entire system thus exhibits *magnetic* responses with well defined resonance frequencies, but its electric polarization is strongly diminished [14,15]. The composite material is then *perfectly* described by the double-layer model shown in Fig. 1(a), with $d = 1.3$ mm being the thickness of the H-pattern (0.1 mm) plus the inner dielectric layer

veal that the PCR cannot reach 1 in the arbitrary incidence case, but the maximum PCR value can still approach 1. As θ increases, we find that the value of ϕ to realize a maximum PCR increases toward 90°, indicating that at glancing incidence we can rotate $\vec{E}$ toward $\hat{x}$ to *maximize* the polarization conversion effect [12]. An opposite behav-
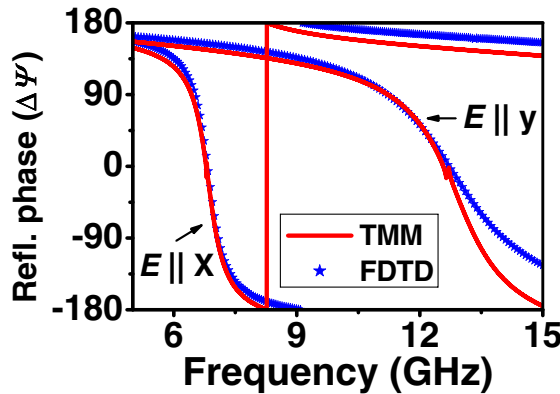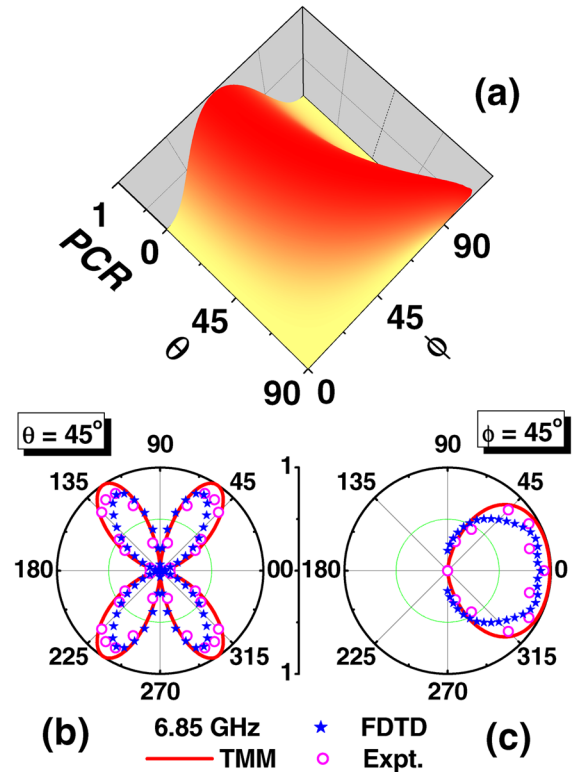

FIG. 4 (color online). Frequency dependences of the reflection phase changes $\Delta\psi_{y(x)}$ on the metamaterial reflector surface for normally incident waves with polarizations $\vec{E}\|\hat{x}$ and $\vec{E}\|\hat{y}$, calculated by TMM on model system (solids lines) and FDTD simulations on realistic structures (solid stars).

FIG. 5 (color online). (a) PCR as a function of θ and ϕ, calculated by TMM. (b) PCR as a function of ϕ with θ fixed as 45°, obtained by TMM (solid lines), FDTD simulation (solid stars), and measurements (open circles). (c) PCR as a function of θ with ϕ fixed as 45°, obtained by TMM (solid lines), FDTD simulations (solid stars) and measurements (open circles). Here, we set $f = 6.85$ GHz.

(1.2 mm) [15]. As a demonstration, we employed FDTD simulations [16,17] to calculate the reflection phase spectra ($\Delta\psi_x(f)$, $\Delta\psi_y(f)$) of the designed composite and showed the results in Fig. 4. The good agreement with the model TMM results supports our conclusions [18].

We fabricated a 497×497 mm^2 sample based on the designs, and performed microwave experiments. As schematically shown in Fig. 1(c), the measurements were carried out in an anechoic chamber using a network analyzer (Agilent 8722 ES) and two linearly polarized horn antennas. The distance between the source/receiver antenna and the sample is 6.9 m. The sample was rotated appropriately to achieve a desired incidence angle (θ, ϕ). Illuminating the sample by a linearly polarized signal with $\vec{E}||\hat{y}_0$ (i.e., s wave [19]), we measured the reflected signal using a $\hat{y}_0$-polarized receiver horn (data collected as $|r_{ss}|^2$) and an $\hat{x}_0$-polarized one (data collected as $|r_{sp}|^2$ [19]). With both $|r_{ss}|^2$ and $|r_{sp}|^2$ obtained, we calculated the PCR and drew the results in Figs. 2(a) and 2(b) as open symbols. We also performed FDTD simulations [17] to calculate the PCR spectra based on the designed system, and showed the results as solid stars in the same figures. *Quantitative* agreements are found among the results obtained by the TMM, the FDTD simulations and experiments. In particular, both experiments and simulations verified the predicted CPC effects. We next employed FDTD simulations to compute the relative phase spectra [$\Delta\varphi_{sp}(f)$], which are again in good agreement with the model TMM results as shown in Fig. 3, indicating that we can obtain any polarization as desired. We finally employed experiments and simulations to study the angle dependences of the polarization conversion effects, and depicted the measured and simulated results in Figs. 5(b) and 5(c). Satisfactory agreements are noted compared with the model TMM results.

Other types of anisotropic metamaterials, say a slab with an anisotropic $\overleftrightarrow{\varepsilon}$ tensor or an anisotropic $\overleftrightarrow{\mu}$ tensor, yield similar polarization manipulation effects. However, such *singe-layer* systems are usually *not* perfectly reflective for EM waves in arbitrary cases, and thus the manipulation efficiency is low. In contrast, our *double-layer* system ensures 100% reflection for arbitrary EM waves, so that the manipulation efficiency is maximized.

In short, we proposed to use metamaterials to manipulate EM wave polarizations, and showed that a *complete conversion* between two perpendicular linear polarizations is realizable under certain conditions. The ideas were successfully demonstrated in the microwave frequency regime by experiments and simulations, and are believed realizable also in higher frequency regimes.

*Corresponding author.
phzhou@fudan.edu.cn

[1] Max Born and Emil Wolf, *Principles of Optics* (Cambridge University Press, Cambridge, England, 1999).
[2] Eugene Hecht, *Optics* (Addison Wesley, New York, 2002).
[3] J. B. Pendry *et al.*, IEEE Trans. Microwave Theory Tech. **47**, 2075 (1999); D. R. Smith *et al.*, Phys. Rev. Lett. **84**, 4184 (2000); D. R. Smith, J. B. Pendry, and M. C. K. Wiltshire, Science **305**, 788 (2004).
[4] R. A. Shelby, D. R. Smith, and S. Schultz, Science **292**, 77 (2001).
[5] D. Sievenpiper *et al.*, IEEE Trans. Microwave Theory Tech. **47**, 2059 (1999); Fan Yang and Y. Rahmat-Samii, IEEE Trans. Antennas Propag. **51**, 2691 (2003); H. Mosallaei and K. Sarabandi, IEEE Trans. Antennas Propag. **52**, 2403 (2004).
[6] A. Figotin and I. Vitebskiy, Phys. Rev. E **68**, 036609 (2003).
[7] Pochi Yeh, *Optical Wave in Layered Media* (Wiley, New York, 1988).
[8] See, e.g., K. Busch, C. T. Chan, and C. M. Soukoulis, in *Photonic Band Gap Materials*, edited by C. M. Soukoulis (Kluwer, Dordrecht, 1996).
[9] Jiaming Hao, Hao Xu, and L. Zhou (unpublished).
[10] For normal incidence, ϕ is meaningless to define the direction of $\vec{k}_{in}$, but is meaningful to differentiate two polarizations. We define that the s-polarized wave has $\vec{E}||(-\sin\phi\hat{x} + \cos\phi\hat{y})$ and the p-polarized one has $\vec{E}||(-\cos\phi\hat{x} + \sin\phi\hat{y})$.
[11] The reflected EM wave can also possess a linear polarization, which is *not* perpendicular to, but rather rotated by an angle with respect to the incident one. For example, in the normal incidence case with $\phi \neq 45°$, the reflected wave still takes a linear polarization when the condition $r_x/r_y = -1$ is met, but the resultant polarization direction, $-E_x\hat{x} + E_y\hat{y}$, is not perpendicular to the original one, $E_x\hat{x} + E_y\hat{y}$, since here $E_x \neq E_y$.
[12] The width ($\delta\phi$) of the *PCR* peak becomes narrower when $\theta \rightarrow 90°$ and reaches zero when $\theta = 90°$.
[13] W. J. Wen *et al.*, Phys. Rev. Lett. **89**, 223901 (2002).
[14] L. Zhou, W. J. Wen, C. T. Chan, and P. Sheng, Appl. Phys. Lett. **83**, 3257 (2003).
[15] J. M. Hao, L. Zhou, and C. T. Chan, Appl. Phys. A **87**, 281 (2007).
[16] K. S. Yee, IEEE Trans. Antennas Propag. **14**, 302 (1966).
[17] CONCERTO 4.0, Vector Fields Limited, England (2004). Limited by the computational power, we studied a smaller system sized 98×98 mm^2 in our simulations.
[18] The double-layer model not only accounts for the reflective properties, but also the surface wave properties of such composite materials (see Ref. [15]).
[19] According to Fig. 1(c), we get $\hat{z}_0 = \sin\theta\cos\phi\hat{x} + \sin\theta\sin\phi\hat{y} + \cos\theta\hat{z}$. Therefore, a wave with $\vec{k}_{in}||\hat{z}_0$, $\vec{E}||\hat{y}_0(\hat{y}_1)$ is s polarized with respect to the sample, and that with $\vec{k}_{in}||\hat{z}_0$, $\vec{E}||\hat{x}_0$ is p polarized.